

Geometric Phase for a Nonstatic Coherent Light-Wave: Nonlinear Evolution Harmonized with the Dynamical Phase

Jeong Ryeol Choi*

*School of Electronic Engineering, Kyonggi University,
Yeongtong-gu, Suwon, Gyeonggi-do 16227, Republic of Korea*

Abstract

Properties of the geometric phase for a nonstatic coherent light-wave arisen in a static environment are analyzed from various angles. The geometric phase varies in a regular nonlinear way, where the center of its variation increases constantly with time. This consequence is due to the effects of the periodic wave collapse and expansion on the evolution of the geometric phase. Harmonization of such a geometric-phase evolution with the dynamical phase makes the total phase evolve with a unique pattern that depends on the degree of nonstaticity. The total phase exhibits a peculiar behavior for the case of extreme nonstaticity, which is that it precipitates periodically in its evolution, owing to a strong response of the geometric phase to the wave nonstaticity. It is confirmed that the geometric phase in the coherent state is mostly more prominent compared to that in the Fock states. For a simple case where the wave nonstaticity disappears, our description of the geometric phase recovers to the well-known conventional one which no longer undergoes periodical change. While the familiar dynamical phase is just related to the expectation value of the Hamiltonian, the geometric phase that we have managed reflects a delicate nonstaticity difference in the evolution of quantum states.

* E-mail: choiardor@hanmail.net

1. INTRODUCTION

Historically, the geometric phase was first recognized in 1931 by Dirac in the form of a path dependent non-integrable phase [1, 2]. A great deal of attention has suddenly been paid to such an extra phase after Berry's seminal report [3, 4] in 1984 in connection with wave functions for dynamical systems with slowly varying parameters. Soon after, Berry's development for a quantum phase has been extended to the case of nonadiabatic wave evolutions by Aharonov and Anandan [5, 6]. Now, the concept of the geometric phase has been further extended to the case of non-cyclic and non-unitary evolutions of the systems including light waves, leading to unveiling the profound features of their quantum nature [7–9].

The geometric phase is a holonomy transformation that reveals geometric character of the wave with a global phase change through its evolution of modulo 2π [10, 11]. A slight different definition of the geometric phase is the geometrical part of the phase evolution for a wave in an arbitrary time t (see, for example, Eq. (4.23) in Ref. [12]). We are interested in this latter definition of the geometric phase in this work, because such a definition enables us to demonstrate nonlinear effects in the evolution of the phase if any.

The geometric phase is noticeable since it directly affects optical phenomena, such as quantum interference, quantum phase transitions, parametric amplification, etc. Furthermore, geometric phase can be applied to many next-generation scientific technologies, including phase gates for holonomic quantum computing [13, 14], detection and grating of a large-angle beam [15], and light control in holograms [16]. In particular, geometric-phase gates in quantum computation allow us to process controllable arithmetic logic operations [14].

If the parameters of a medium vary in time, a light wave in that medium may become nonstatic. In a previous work [17], we have shown that nonstatic quantum light waves can also appear even in a static environment. We have investigated nonstatic quantum light waves and their associated phase properties in the Fock states [17–19]. Subsequently, that research was extended to the nonstatic waves in the coherent state [20]. Such waves exhibit a collapse and expansion in turn in time as their characteristic of nonstaticity. In those cases, a node and an

antinode take place periodically in the graphic of the time evolution of waves in the quadrature space.

Consequently, the eigenfunctions associated with the nonstatic waves are time-varying, i.e., they are represented in terms of a time function that obeys a nonlinear differential equation. It was shown that such a variation of the eigenfunctions in the Fock states leads to the appearance of a geometric phase as the manifestation of peculiar wave nonstaticity [18]. If we think that the geometric phase (latter definition) does not emerge in the ordinary Fock-state waves described by the simple harmonic oscillator [21–24], such a result in that work is worthy of note.

In this work, we will investigate the geometric phase for a nonstatic light wave arisen in a static environment through the same sprit of Ref. [18], but in the coherent state [25, 26]. The importance of coherent states is that it is possible to manage the correlation and coherence properties of light waves by means of them. The preservation and enhancement of quantum coherence is needed in fulfilling quantum algorithms in quantum computation with qubits. We elucidate the relation between nonstatic-wave mechanism and its resultant geometric phase in the coherent state through this research. To get a keen insight for the kinematics of the phase evolution with nonstaticity, the clarification of the behavior of accompanying geometric phases is indispensable.

The effects of the periodic wave collapse and expansion on the evolution of the considered geometric phase will be analyzed. Similarities and differences of our consequence for the phase evolution in the coherence state and that in the Fock states will be shown. The geometric phase will also be compared to the ordinary dynamical phase and we clarify their interplay and concurrent relation with harmony for the formation of a novel phase outcome. Phase properties with an extreme nonstaticity will be additionally seen. Through these, we deepen the understanding for the characteristics of the quantum phase in general nonstatic coherent waves and demonstrate the geometrical features of the wave evolution.

2. DESCRIPTION OF THE NONSTATIC COHERENT STATE

Let us consider a nonstatic light wave in a non-dissipative medium where the electric permit-

tivity ϵ and magnetic permeability μ are independent of time. To investigate the geometric phase strictly, we need to develop a theory for the phenomena of quantum coherent wave with nonstaticity together with the structure of the related quantum state. The Hamiltonian which describes light-wave evolution in the medium is given by

$$\hat{H} = \hat{p}^2/(2\epsilon) + \epsilon\omega^2\hat{q}^2/2, \quad (1)$$

where \hat{q} is the operator representation of the canonical variable $q(t)$ that gives amplitude of the wave and $\hat{p} = -i\hbar\partial/\partial q$. $q(t)$ in this setup corresponds to the time function in the vector potential when we separate it into time and position functions in the Coulomb gauge [17, 20]. The angular frequency ω of the wave satisfies $\omega = kc$ where k is the wave number, whereas the velocity of the wave is expressed as $c = 1/\sqrt{\epsilon\mu}$. If we denote a general classical solution for the variable q as $Q_{\text{cl}}(t)$, it can be represented in the form

$$Q_{\text{cl}}(t) = Q_0 \cos \tilde{\theta}(t), \quad (2)$$

where Q_0 is a constant, $\tilde{\theta}(t) = \omega(t - t_0) + \theta_0$, t_0 is an initial time, and θ_0 is an arbitrary phase at t_0 . We consider only the case where $t \geq t_0$ for convenience throughout this work.

A nonstatic wave is described by a time function of the form [17, 20]

$$f(t) = c_1 \sin^2 \tilde{\varphi}(t) + c_2 \cos^2 \tilde{\varphi}(t) + c_3 \sin[2\tilde{\varphi}(t)], \quad (3)$$

where $\tilde{\varphi}(t) = \omega(t - t_0) + \varphi$ and φ is a phase at $t = t_0$, while c_1 , c_2 , and c_3 are real constants which give the nonstaticity and they satisfy the relation

$$c_1 c_2 - c_3^2 = 1, \quad (4)$$

with

$$c_1 c_2 \geq 1. \quad (5)$$

A generalized annihilation operator associated with the nonstatic light is represented as [20]

$$\hat{A} = \sqrt{\frac{\epsilon\omega}{2\hbar f(t)}} \left(1 - i \frac{\dot{f}(t)}{2\omega} \right) \hat{q} + i \sqrt{\frac{f(t)}{2\epsilon\omega\hbar}} \hat{p}. \quad (6)$$

The Hermitian adjoint of this operator \hat{A}^\dagger is the creation operator, whereas the two operators satisfy the boson commutation relation such that $[\hat{A}, \hat{A}^\dagger] = 1$. We write the eigenvalue equation for \hat{A} in the form

$$\hat{A}|A\rangle = A|A\rangle, \quad (7)$$

where A is the eigenvalue and $|A\rangle$ is the eigenfunction. Then, $|A\rangle$ is a generalization of the coherent state considering nonstaticity. If we set

$$\hat{I} = \hbar\omega(\hat{A}^\dagger\hat{A} + 1/2), \quad (8)$$

\hat{I} is an invariant operator [20]. While the Hamiltonian itself (\hat{H}) is also an invariant operator, \hat{I} is regarded as a generalized invariant operator and is reduced to \hat{H} when $c_1 = c_2 = 1$ and $c_3 = 0$.

Before we enter the nonstatic coherent state, let us look into the nonstatic Fock states as a preliminary step. The Fock-state wave functions with nonstaticity are given by [17]

$$\langle q|\Psi_n(t)\rangle = \langle q|\Phi_n(t)\rangle \exp[i\gamma_n(t)] \quad n = 0, 1, 2, \dots, \quad (9)$$

where the associated eigenfunctions $\langle q|\Phi_n(t)\rangle$ and phases $\gamma_n(t)$ are expressed as

$$\langle q|\Phi_n(t)\rangle = \left(\frac{\zeta(t)}{\pi}\right)^{1/4} \frac{1}{\sqrt{2^n n!}} H_n\left(\sqrt{\zeta(t)}q\right) \exp\left[-\frac{1}{2}\zeta(t)\left(1 - i\frac{\dot{f}(t)}{2\omega}\right)q^2\right], \quad (10)$$

$$\gamma_n(t) = -\omega(n + 1/2) \int_{t_0}^t f^{-1}(t') dt' + \gamma_n(t_0), \quad (11)$$

while H_n are n th order Hermite polynomials and $\zeta(t) = \epsilon\omega/[\hbar f(t)]$. All the states which retain their functional form during nonstatic evolution can be represented as a superposition of $\langle q|\Psi_n(t)\rangle$ such that

$$\langle q|\Psi(t)\rangle = \sum_{n=0}^{\infty} a_n \langle q|\Psi_n(t)\rangle, \quad (12)$$

where a_n are complex numbers that obey $\sum_{n=0}^{\infty} |a_n|^2 = 1$. Interference between the phases of different components in Eq. (12) is responsible for the emergence of nonclassical effects in the resultant state, such as oscillation in photon-number distribution [27], quadrature squeezing

[28], and sub-Poissonian photon statistics [29]. The generalized coherent state $\langle q|A\rangle$ that we are interested in this work can also be represented in a similar way. Namely [30],

$$\langle q|A\rangle = \sum_{n=0}^{\infty} b_n(A) \langle q|\Phi_n\rangle, \quad (13)$$

where the transformation functions are given by $b_n(A) = \exp(-|A|^2/2)A^n/\sqrt{n!}$. Although we have represented Eq. (13) in a slightly different manner compared to Eq. (12), the full wave function in the coherent state, which includes its phase, can also be represented as Eq. (12), i.e., can be expressed as an expansion in terms of $\langle q|\Psi_n(t)\rangle$ (see Appendix A).

The coherent state that has nonstatic characteristic was derived using Eq. (7) in our previous work which is Ref. [20]. The resultant eigenfunction in the configuration space is of the form

$$\langle q|A\rangle = \sqrt[4]{\frac{\zeta(t)}{\pi}} \exp\left[-\frac{\zeta(t)}{2}\left(1-i\frac{\dot{f}(t)}{2\omega}\right)q^2 + \sqrt{2\zeta(t)}Aq - \frac{1}{2}|A|^2 - \frac{1}{2}A^2\right]. \quad (14)$$

Though this state exhibits nonstaticity, it is overcomplete and non-orthogonal as usual coherent states. On the other hand, the eigenvalue associated to this state is given by [20]

$$A(t) = A_0 e^{-i[\omega T(t)+\theta]}, \quad (15)$$

where A_0 is its amplitude, which is of the form

$$A_0 = \left\{ \frac{\epsilon\omega}{2\hbar} \left[\frac{\cos^2 \tilde{\theta}(t)}{f(t)} + \left(\frac{\dot{f}(t)}{2\omega\sqrt{f(t)}} \cos \tilde{\theta}(t) + \sqrt{f(t)} \sin \tilde{\theta}(t) \right)^2 \right] \right\}^{1/2} Q_0, \quad (16)$$

while θ is the phase of $A(t)$ at t_0 , and

$$T(t) = G(t) - G(t_0) + \mathcal{G}(t)/\omega, \quad (17)$$

with

$$G(\tau) = \frac{1}{\omega} \tan^{-1} \{ c_3 + c_1 \tan[\omega(\tau - t_0) + \varphi] \}, \quad (18)$$

$$\mathcal{G}(t) = \pi \sum_{m=0}^{\infty} u[t - t_0 - (2m+1)\pi/(2\omega) + \varphi/\omega], \quad (19)$$

whereas $u[x]$ is the Heaviside step function. We note that A_0 is a time constant, but dependent on c_1 , c_2 , φ , and θ_0 . In the expression of Eq. (17) with Eqs. (18) and (19), we have restricted

the region of φ as $-\pi/2 \leq \varphi < \pi/2$ for convenience without loss of generality. This interval is enough because the geometric phase varies with the period π for φ . In fact, $T(t)$ can also be represented as [20]

$$T(t) = \int_{t_0}^t f^{-1}(t') dt'. \quad (20)$$

The magnitude of nonstaticity for a wave can be estimated by a measure of nonstaticity. For the coherent state, Eq. (14), such a measure is determined by c_1 and c_2 such that [17, 20]

$$D = \frac{\sqrt{(c_1 + c_2)^2 - 4}}{2\sqrt{2}}. \quad (21)$$

This is the same as the nonstaticity measure in the Fock states.

The coherent state described up until now can be applied to the analysis of the system. For instance, let us see the behavior of \hat{I} and \hat{H} in the coherent state. Though \hat{I} and \hat{H} do not vary over time, we see from Fig. 1 that their expectation values are dependent on c_1 and c_2 . Figure 1(a) is the case where $\langle A|\hat{I}|A\rangle$ is smaller than $\langle A|\hat{H}|A\rangle$, whereas Fig. 1(b) the case where $\langle A|\hat{I}|A\rangle$ is larger than $\langle A|\hat{H}|A\rangle$. The difference of $\langle A|\hat{I}|A\rangle$ from $\langle A|\hat{H}|A\rangle$ becomes large as c_1 and/or c_2 increase in most cases, but $\langle A|\hat{I}|A\rangle$ is reduced to $\langle A|\hat{H}|A\rangle$ in the limit $c_1 = c_2 \rightarrow 1$.

The wave description developed until now in the coherent state is also necessary in evaluating phases of the nonstatic light, because the characteristics of the geometric phase are determined depending on the specific formula of wave functions. The geometric phase of the nonstatic quantum light wave will be investigated in the following sections using that description.

3. GENERALIZED NONLINEAR GEOMETRIC PHASE

3.1. Integral Representation

We focus on the geometric phase that takes place due to nonstaticity in the wave evolutions of quantum light. Several mathematical methods for formulating geometric phases are known. Some of them are the methods utilizing the Schrödinger equation [10, 31], a path integral technique [32–34], and the canonical transformation approach [35, 36]. The former method (the method based on the Schrödinger equation) is much more general than others and usually

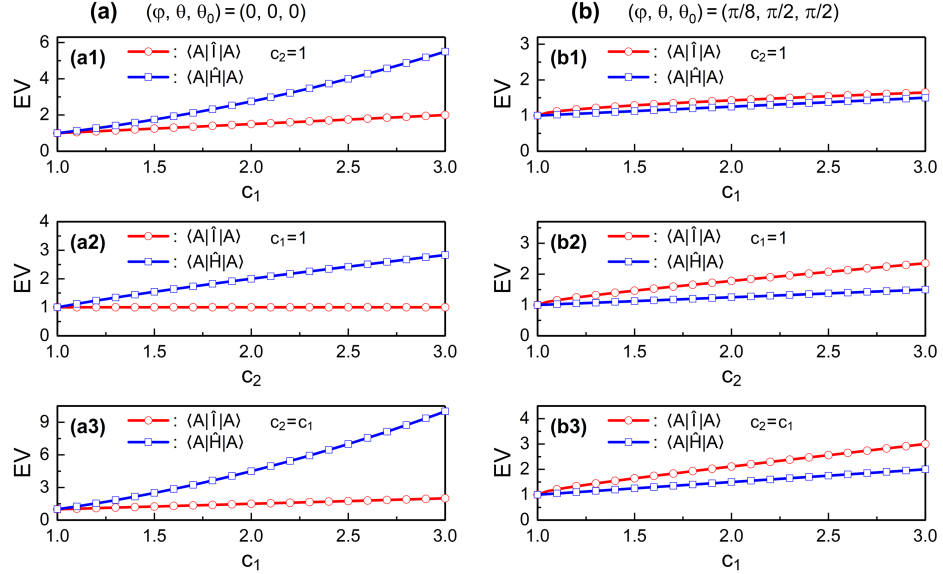


FIG. 1: (a) is the relation of the expectation value (EV) of \hat{I} ($\langle A|\hat{I}|A\rangle$) and \hat{H} ($\langle A|\hat{H}|A\rangle$) with c_1 (a1, a3) and c_2 (a2) in the coherent state, where angles are chosen as $(\varphi, \theta, \theta_0) = (0, 0, 0)$: we have taken $c_2 = 1$ for (a1), $c_1 = 1$ for (a2), and $c_2 = c_1$ for (a3). (b) is the same as (a), but for the case of a different angles choice which is $(\varphi, \theta, \theta_0) = (\pi/8, \pi/2, \pi/2)$. c_3 is determined based on the values of c_1 and c_2 according to Eq. (4). Among two possible values of c_3 which are $c_3 = \pm\sqrt{c_1c_2 - 1}$, we have chosen $c_3 = \sqrt{c_1c_2 - 1}$ in this figure for convenience: this convention will also be used for all subsequent figures. We have used $t = 1$, $t_0 = 0$, $Q_0 = 1$, $\omega = 1$, $\hbar = 1$, and $\epsilon = 1$. The EV $\langle A|\hat{I}|A\rangle = \hbar\omega(A_0^2 + 1/2)$, depicted here, is evaluated based on Eq. (8) with the eigenvalue relation Eq. (7), utilizing the formula of $A(t)$ given in Eq. (15) and its complex conjugate $A^*(t)$ which are described with Eqs. (16)-(19). The formula of $\langle A|\hat{H}|A\rangle$ is also evaluated with the same procedure using Eq. (1), after converting (\hat{q}, \hat{p}) in the Hamiltonian into the expression with $(\hat{A}, \hat{A}^\dagger)$ based on Eq. (6) and its Hermitian-conjugate representation.

adopted in the relevant studies owing to its simplicity. We will also use it in the present work.

In Ref. [18], we have studied the properties of the geometric phases for nonstatic waves in the Fock states as mentioned previously. The geometric phase for a superposition of Fock states, including coherent states, can also be derived in the same way adopted in that report.

Hence, it is possible to extend the method given in Ref. [18] to our coherent state through the expression given in Eq. (13). However, since the wave function in the coherent state is known in Eq. (14) at this stage, the use of that wave function instead of Eq. (13) is more convenient for the derivation of the associated geometric phase.

Bearing in mind this, let us evaluate the geometric phase of the nonstatic light, in addition to the usual dynamical phase, in the coherent state. The definitions of the geometric and dynamical phases are given by

$$\gamma_G(t) = \int_{t_0}^t \langle A(t') | i \frac{\partial}{\partial t'} | A(t') \rangle dt' + \gamma_G(t_0), \quad (22)$$

$$\gamma_D(t) = -\frac{1}{\hbar} \int_{t_0}^t \langle A(t') | \hat{H}(\hat{q}, \hat{p}, t') | A(t') \rangle dt' + \gamma_D(t_0). \quad (23)$$

If we think that Eq. (22) includes a time derivative of the eigenfunction, the geometric phase occurs only when the eigenfunction is described in terms of time [24]. The geometric phase defined in Eq. (22) is gauge-invariant: an exemplary proof of this characteristic is shown in Appendix B. Because the nonstatic eigenfunction given in Eq. (14) is dependent on time, the geometric phase in this coherent-state description is non-zero. The time derivative of the eigenfunction, Eq. (14), in the configuration space yields

$$\begin{aligned} \frac{\partial \langle q | A \rangle}{\partial t} = & \left[\frac{i\omega}{f(t)} A^2 - \frac{\dot{f}(t)}{4f(t)} - \sqrt{2\zeta(t)} \frac{A}{f(t)} \left(\frac{\dot{f}(t)}{2} + i\omega \right) q \right. \\ & \left. + \left(\frac{i\epsilon}{8\hbar f^2(t)} [2\omega - i\dot{f}(t)]^2 - \frac{i\epsilon\omega^2}{2\hbar} \right) q^2 \right] \langle q | A \rangle. \end{aligned} \quad (24)$$

A rigorous evaluation of Eq. (22) after inserting this formula gives

$$\gamma_G(t) = \int_{t_0}^t \Gamma_G(t') dt' + \gamma_G(t_0), \quad (25)$$

where

$$\Gamma_G(t) = \frac{\omega}{4} g_1(t) + \frac{1}{16\omega} g_2(t) + \frac{1}{4} g_3(t) + \frac{\omega}{4} g_4(t), \quad (26)$$

while $g_i(t)$ ($i = 1-4$) are time functions that are represented as (see Appendix C)

$$g_1(t) = -\frac{1}{f(t)} \{ 2A_0^2 \cos[2(\omega T(t) + \theta)] - 2A_0^2 + 1 \}, \quad (27)$$

$$g_2(t) = \frac{[\dot{f}(t)]^2}{f(t)} \{2A_0^2 \cos[2(\omega T(t) + \theta)] + 2A_0^2 + 1\}, \quad (28)$$

$$g_3(t) = -\frac{2\dot{f}(t)}{f(t)} A_0^2 \sin[2(\omega T(t) + \theta)], \quad (29)$$

$$g_4(t) = f(t) \{2A_0^2 \cos[2(\omega T(t) + \theta)] + 2A_0^2 + 1\}. \quad (30)$$

For the non-displaced case where $A_0 = 0$, Eq. (25) is reduced to

$$\gamma_G(t) = \frac{1}{4} \int_{t_0}^t \left(\omega f(t') - \frac{\omega}{f(t')} + \frac{[\dot{f}(t')]^2}{4\omega f(t')} \right) dt' + \gamma_G(t_0). \quad (31)$$

This is the same as the geometric phase in the Fock states with $n = 0$ (see Eqs. (9)-(13) in Ref. [18]). This correspondence is natural because the coherent state is the displaced one of the zero-point Fock state.

3.2. Analytical Formula of Geometric Phase

3.2.1. Deriving geometric phase

Direct acquisition of the geometric phase from Eq. (25) may be not easy because it involves a complicated integration. Our strategy for overcoming this difficulty is that we turn our attention to the dynamical phase for the moment, which seems less hard, and therein we completely derive it. Then we represent the geometric phase in terms of the factor(s) used in the dynamical phase, expecting that this manipulation leads to full representation of the geometric phase in a reasonable way. To obtain the dynamical phase, we insert the Hamiltonian Eq. (1) into Eq. (23) after expressing the canonical variables in terms of the ladder operators \hat{A} and \hat{A}^\dagger . Then, using Eqs. (7) and (15), we get

$$\gamma_D(t) = \int_{t_0}^t \Gamma_D(t') dt' + \gamma_D(t_0), \quad (32)$$

where

$$\Gamma_D(t) = -\left(\frac{\omega}{4} \bar{g}_1(t) + \frac{1}{16\omega} g_2(t) + \frac{1}{4} g_3(t) + \frac{\omega}{4} g_4(t) \right), \quad (33)$$

while (see Appendix C)

$$\bar{g}_1(t) = -\frac{1}{f(t)} \{2A_0^2 \cos[2(\omega T(t) + \theta)] - 2A_0^2 - 1\}. \quad (34)$$

As can be seen from Appendix D, $\Gamma_D(t)$ is a time constant though it is expressed in terms of time. Because Eq. (23) means that $\Gamma_D(t)$ is directly related to the expectation value of \hat{H} , this consequence is not strange and closely related to the energy conservation law. Since $\Gamma_D(t)$ does not vary over time, we can write Eq. (32) without the integral symbol in the form

$$\gamma_D(t) = \Gamma_D(\bar{t})[t - t_0] + \gamma_D(t_0), \quad (35)$$

where \bar{t} is an arbitrary fixed time that satisfies $\bar{t} \geq t_0$. The time fixation $t = \bar{t}$ in Γ_D is not a necessary condition in the above equation, but the related mathematics becomes simpler by treating Eq. (35) with such a fixed time.

Now, in the case of the geometric phase, we take attention to the fact that Eq. (26) can be rearranged in a way that it involves $\Gamma_D(t)$ such that

$$\Gamma_G(t) = -\frac{\omega}{2f(t)} - \Gamma_D(t). \quad (36)$$

Hence, employing again the fact that $\Gamma_D(t)$ is constant over time together with the relation in Eq. (20), the geometric phase described in terms of Eq. (36) can also be reduced to a simple form as

$$\gamma_G(t) = -\frac{1}{2}\omega T(t) - \Gamma_D(\bar{t})[t - t_0] + \gamma_G(t_0). \quad (37)$$

Because we know not only the formula of $T(t)$ in the above equation from Eq. (17) with Eqs. (18) and (19), but the formula of $\Gamma_D(\bar{t})$ from Eq. (33) with Eqs. (34), (28), (29), and (30) as well, we now have identified the complete analytical formula of the geometric phase in the coherent state. This formula is more general than the existing ones [35, 37] concerning the coherent state. We note that the geometric phase appeared in the previous reports (Refs. [35, 37]) is the one that does not consider the wave nonstaticity. The geometric phase given in Eq. (37) exhibits nonlinear effects due to the wave nonstaticity. By the way, it is impossible to gauge out the geometric part in phase because of the fact that the geometric phase is gauge invariant.

If we take $c_1 = c_2 = 1$ and $c_3 = 0$, the nonlinear effects in the geometric phase vanish, leading to the geometric phase being a reduced familiar one:

$$\gamma_G(t) = \omega A_0^2(t - t_0) + \gamma_G(t_0), \quad (38)$$

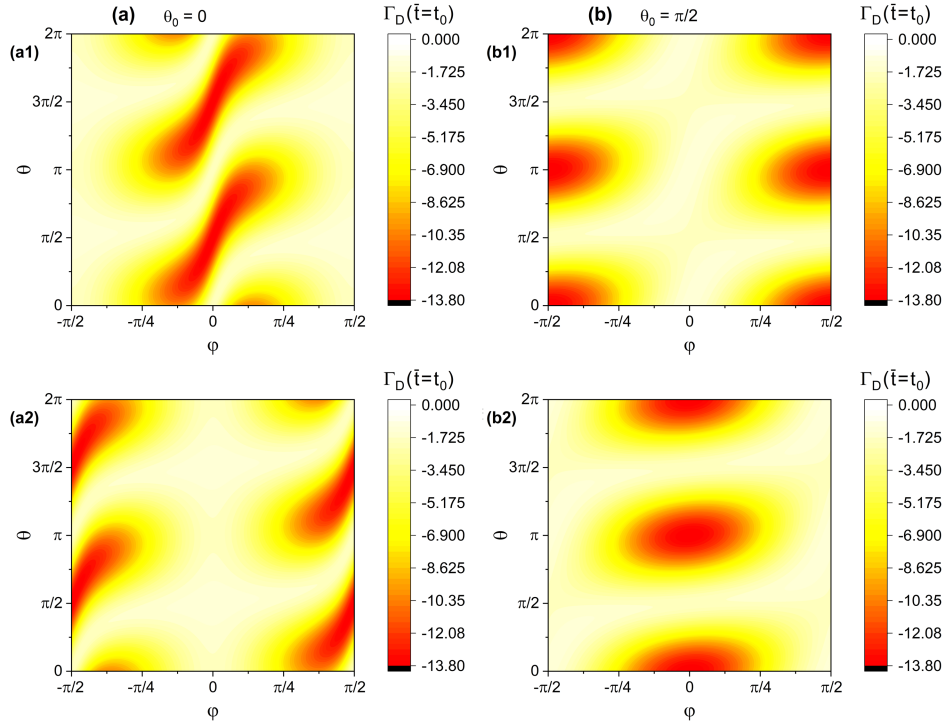


FIG. 2: Density plots of $\Gamma_D(\bar{t} = t_0)$ as a function of φ and θ , where Eq. (39) with Eqs. (16), (40), and (41) is used as its formula. We have chosen $\theta_0 = 0$ for (a) and $\theta_0 = \pi/2$ for (b), whereas (c_1, c_2) are taken as (5.0, 0.2) for subpanels (a1) and (b1), and as (0.2, 5.0) for (a2) and (b2). We have used $Q_0 = 1$, $\omega = 1$, $\epsilon = 1$, and $\hbar = 1$.

which coincides with the formula given in Ref. [38]. If the displacement of the quadrature oscillation also disappears ($A_0 \rightarrow 0$) along with this, the geometric phase no longer exists. We can thereby conclude that there are two sources of the appearing of the geometric phase for the present case. One is the wave nonstaticity and the other is the displacement of the oscillation. On the other hand, the case of Fock states treated in Refs. [17, 18], the origin of the geometric phase is only the wave nonstaticity.

3.2.2. Characteristics of $\Gamma_D(\bar{t})$

Because the geometric phase is represented in terms of $\Gamma_D(\bar{t})$, it is important to elucidate the characteristics of $\Gamma_D(\bar{t})$. If we take $\bar{t} = t_0$ without loss of generality under the condition given

in Eq. (4), $\Gamma_D(\bar{t})$ becomes

$$\begin{aligned}\Gamma_D(\bar{t} = t_0) = & -\frac{\omega}{16\kappa_1} [4(1 + 4A_0^2 \sin^2 \theta) + (1 + 4A_0^2 \cos^2 \theta)(4\kappa_1^2 + \kappa_2^2) \\ & - 8A_0^2 \sin(2\theta)\kappa_2],\end{aligned}\quad (39)$$

where

$$\kappa_1 = c_1 \sin^2 \varphi + c_2 \cos^2 \varphi + \sqrt{c_1 c_2 - 1} \sin(2\varphi), \quad (40)$$

$$\kappa_2 = (c_1 - c_2) \sin(2\varphi) + 2\sqrt{c_1 c_2 - 1} \cos(2\varphi). \quad (41)$$

$\Gamma_D(\bar{t})$ in Eq. (39) is universally valid since the choice of \bar{t} does not affect the result. Figure 2 represents the relation of $\Gamma_D(\bar{t} = t_0)$ on angles φ , θ , and θ_0 . We confirm from each panel of this figure that $\Gamma_D(\bar{t} = t_0)$ is different depending on φ and θ in a regular manner; moreover, the comparison between subpanels (a1) and (b1) (or (a2) and (b2)) shows that $\Gamma_D(\bar{t} = t_0)$ also depends on θ_0 . Additional comparison between (a1) and (a2) (or (b1) and (b2)) shows the difference of $\Gamma_D(\bar{t} = t_0)$ depending on c_1 and c_2 . Meanwhile, the magnitude of $\Gamma_D(\bar{t})$ can be regulated at our will by adjusting the value of Q_0 (or A_0 instead). This regulation does not affect the measure of nonstaticity since the measure is determined only by c_1 and c_2 as can be confirmed from Eq. (21).

If we further take $\varphi = \theta = 0$, Eq. (39) is simplified to

$$\Gamma_D(\bar{t} = t_0) = -\omega \left[\frac{c_1 + c_2}{4} + A_0^2 \left(c_1 + c_2 - \frac{1}{c_2} \right) \right]. \quad (42)$$

For the static case ($c_1 = c_2 = 1$), this becomes

$$\Gamma_D(\bar{t} = t_0) = -\omega \left(A_0^2 + \frac{1}{2} \right). \quad (43)$$

By the way, for the comparison purpose, we have represented the consequence of wave phases in the Fock states in Appendix E. The formula in Eq. (43) is similar to the following familiar form in the Fock states, which can be obtained from Eq. (E2) in Appendix E with the same choice of the nonstaticity parameters, $c_1 = c_2 = 1$:

$$\frac{\gamma_{D,n}(t) - \gamma_{D,n}(t_0)}{t - t_0} = -\omega \left(n + \frac{1}{2} \right). \quad (44)$$

It looks like that A_0^2 in Eq. (43) plays the same role as n in Eq. (44). This fact will be used in the later investigation.

3.3. Total Phase and Nonlinearity Perspectives

The total phase acquired by the state in the course of its evolution is the sum of the geometric and dynamical phases:

$$\gamma(t) = \gamma_G(t) + \gamma_D(t) = -\frac{1}{2}\omega T(t) + \gamma(t_0), \quad (45)$$

where $\gamma(t_0)$ is the phase at t_0 . This is the same as the minimum evolution of the overall phase for the light in the Fock states, i.e., the value of Eq. (45) is identical to that in the Fock states with the zero-point quantum number ($n = 0$), which appears in Eq. (E3) in Appendix E.

Regarding the phase shown in Eq. (45), the wave function in the coherent state is given by

$$\langle q | \Psi_{\text{coh}}(t) \rangle = \langle q | A \rangle e^{i\gamma(t)}. \quad (46)$$

It may be possible to investigate the complete nonstatic effects of the displaced wave utilizing this generalized wave function from the theoretical point of view.

By the way, it may be instructive to represent $\gamma_G(t)$ and $\gamma(t)$ in the forms

$$\gamma_G(t) = \gamma_{G,\text{NL}}(t) + \gamma_{G,\text{L}}(t), \quad (47)$$

$$\gamma(t) = \gamma_{\text{NL}}(t) + \gamma_{\text{L}}(t), \quad (48)$$

where $\gamma_{G,\text{NL}}(t)$ and $\gamma_{\text{NL}}(t)$ are periodical nonlinear terms whereas $\gamma_{G,\text{L}}(t)$ and $\gamma_{\text{L}}(t)$ are linear terms, which are given by

$$\gamma_{G,\text{NL}}(t) = \gamma_{\text{NL}}(t) = -\frac{1}{2}\omega[T(t) - (t - t_0)] + \gamma_{G,\text{NL}}(t_0), \quad (49)$$

$$\gamma_{G,\text{L}}(t) = -\left(\Gamma_D(\bar{t}) + \frac{1}{2}\omega\right)(t - t_0) + \gamma_{G,\text{L}}(t_0), \quad (50)$$

$$\gamma_{\text{L}}(t) = -\frac{1}{2}\omega(t - t_0) + \gamma_{\text{L}}(t_0), \quad (51)$$

together with the trivial relation $\gamma_{\text{NL}}(t_0) = \gamma_{G,\text{NL}}(t_0)$. Nonlinear effects taken place by the nonlinear terms given above are apparently a matter of concern and interest. Nonlinearity in

the geometric phase and its consequence in relation with the total phase will be investigated in detail in Sec. 5.

4. COMPLETENESS OF THE GENERAL GEOMETRIC PHASE

The geometric phase given in Eq. (37) (or its non-integrated formula in Eq. (25)) is a generalized one regarding wave nonstaticity of the coherent state, whereas it is reduced to the well-known standard one when $c_1 = c_2 \rightarrow 1$. We will now see the validity and completeness of such a geometric phase by examining whether the full wave function developed considering it obeys the Schrödinger equation or not. By taking time derivative of the wave function, Eq. (46), after inserting Eqs. (14) and (45) with Eq. (15) in it, we obtain

$$\frac{\partial \langle q | \Psi_{\text{coh}}(t) \rangle}{\partial t} = \frac{e^{V(t)}}{4\hbar f^2(t)} \sqrt[4]{\frac{\zeta(t)}{\pi}} [W(t)q^2 - X(t)q - Y(t)], \quad (52)$$

where

$$\begin{aligned} V(t) = & \sqrt{2\zeta(t)} A_0 e^{-i(\omega T + \theta)} q - \{A_0^2(1 + e^{-2i(\omega T + \theta)}) + 4i\theta + 5i\omega T \\ & + \zeta(t)[1 - i\dot{f}(t)/(2\omega)]q^2\}/2, \end{aligned} \quad (53)$$

$$W(t) = \{2\omega\dot{f}(t) - i[\dot{f}(t)]^2 + i f(t)\ddot{f}(t)\}e^{2i(\omega T + \theta)}\epsilon, \quad (54)$$

$$X(t) = 2\sqrt{2\zeta(t)}\hbar A_0 e^{i(\omega T + \theta)}[f(t)\dot{f}(t) + 2i\omega f^2(t)\dot{T}], \quad (55)$$

$$Y(t) = e^{2i(\omega T + \theta)}\hbar f(t)\dot{f}(t) + 2i\hbar\omega f^2(t)\dot{T}[e^{2i(\omega T + \theta)} - 2A_0^2]. \quad (56)$$

We used the relation $dA_0/dt = 0$ in this evaluation, but did/need not resort to the formula of A_0 given in Eq. (16) in this case. On the other hand, the second order differentiation of the wave function with respect to q is of the form

$$\begin{aligned} \frac{\partial^2 \langle q | \Psi_{\text{coh}}(t) \rangle}{\partial q^2} = & \sqrt[4]{\frac{\zeta(t)}{\pi}} e^{-Z(t)/2} \{ \{ \sqrt{2\zeta(t)} A_0 e^{-i(\omega T + \theta)} - \zeta(t)[1 - i\dot{f}(t)/(2\omega)]q \}^2 \\ & - \zeta(t)[1 - i\dot{f}(t)/(2\omega)] \}, \end{aligned} \quad (57)$$

where

$$Z(t) = A_0^2(1 + e^{-2i(\omega T + \theta)}) - 2\sqrt{2\zeta(t)} A_0 e^{-i(\omega T + \theta)} q + i\omega T + \zeta(t)[1 - i\dot{f}(t)/(2\omega)]q^2. \quad (58)$$

Now we regard the following relations:

$$\dot{T} = 1/f(t), \quad (59)$$

$$\ddot{f}(t) = \frac{[\dot{f}(t)]^2}{2f(t)} - 2\omega^2[f(t) - 1/f(t)]. \quad (60)$$

The relation in Eq. (59) can be recognized from Eq. (20). Another relation, Eq. (60), is shown in Eq. (3) of Ref. [20]. By utilizing Eqs. (52) and (57) after inserting Eqs. (59) and (60) into Eq. (52), it is possible to confirm that the wave function satisfies the Schrödinger equation such that

$$i\hbar \frac{\partial \langle q | \Psi_{\text{coh}}(t) \rangle}{\partial t} = -\frac{\hbar^2}{2\epsilon} \frac{\partial^2 \langle q | \Psi_{\text{coh}}(t) \rangle}{\partial q^2} + \frac{1}{2} \epsilon \omega^2 q^2 \langle q | \Psi_{\text{coh}}(t) \rangle. \quad (61)$$

Thus, the total phase that we have considered is correct. This result also means that its components, the geometric phase (and the dynamical phase), are exactly evaluated, demonstrating that our geometric phase for the nonstatic wave is right. We note that the wave functions in Fock states given in Eq. (9) also explicitly satisfy the Schrödinger equation [17].

The consequence in Eq. (61) is not surprising, but is due on account of the fact that the phases in Eqs. (22) and (23) are defined via the use of the Schrödinger equation. Let us briefly check about this. The substitution of the wave function $|\Psi_{\text{coh}}(t)\rangle$ in Eq. (46) into the Schrödinger equation gives

$$|A\rangle \dot{\gamma}(t) = i \frac{\partial |A\rangle}{\partial t} - \frac{\hat{H}}{\hbar} |A\rangle. \quad (62)$$

By operating $\langle A|$ in each side in the above equation from left and taking an integration with respect to t , we have

$$\begin{aligned} \gamma(t) - \gamma(t_0) &= \int_{t_0}^t \langle A(t') | i \frac{\partial}{\partial t'} | A(t') \rangle dt' \\ &\quad - \frac{1}{\hbar} \int_{t_0}^t \langle A(t') | \hat{H}(\hat{q}, \hat{p}, t') | A(t') \rangle dt'. \end{aligned} \quad (63)$$

We see that the first term in the right-hand side of the above equation is the geometric phase accumulated during a time interval $t - t_0$, whereas the second term is the dynamical phase evolved at the same time. Although the total phase follows the Schrödinger equation in this way, such compliance requires the relation in Eq. (60) as a necessary condition: one can easily confirm that the adopted time function $f(t)$, Eq. (3), satisfies this condition exactly.

The theory of nonstatic waves along this line has been developed based on the fact that the associated wave functions in Fock, coherent, and other quantum states evolve in time as per the Schrödinger equation. Such evolutions in a static environment require the emergence or modification of the geometric phase in the wave. The phase $\gamma(t)$ is often neglected in the representation of the coherent wave because it does mostly not affect the expectation value of an observable. For instance, recent studies for the coherent states in Refs. [20, 39, 40] are the cases where $\gamma(t)$ is not considered. However, $\gamma(t)$ and the geometric phase as its component play crucial roles in some cases such as wave interferences and quantum superpositions. The geometry-oriented phase difference in the interference experiment is non-intuitive in many cases and can only be understood via the geometric phase perspective. Interpretation of shifts in the location of the wave maximum for superposed waves, which are caused by geometric phase, demands a rigorous analysis in general.

5. ANALYSIS OF THE BEHAVIOR OF GEOMETRIC PHASE

5.1. Nonlinear Characteristics

We now clarify the influence of wave nonstaticity on phase evolutions by analyzing the evolution of the geometric phase and its relation with the dynamical phase together with their collaborative formation of the resultant overall phase. The time evolution of the geometric phase, the dynamical phase, and the overall phase are plotted in Fig. 3 for several different values of ω . Roughly speaking, the geometric phase increases with time, while the dynamical phase decreases. Because the absolute value of the dynamical phase is greater than the geometric phase, the total phase decreases. The increase of the geometric phase is more rapid when ω is large.

While the previously reported geometric phase [35, 37] in the coherent state, which is the same as Eq. (38), increases monotonically over time, the geometric phase in this work fluctuates as time goes by provided that $f(t) \neq 1$. This is purely due to the effects of the wave nonstaticity on the evolution of the geometric phase. From a careful analysis of panel (a) in Fig. 3, we see that the geometric phase abruptly drops whenever the wave forms a node in its evolution in the

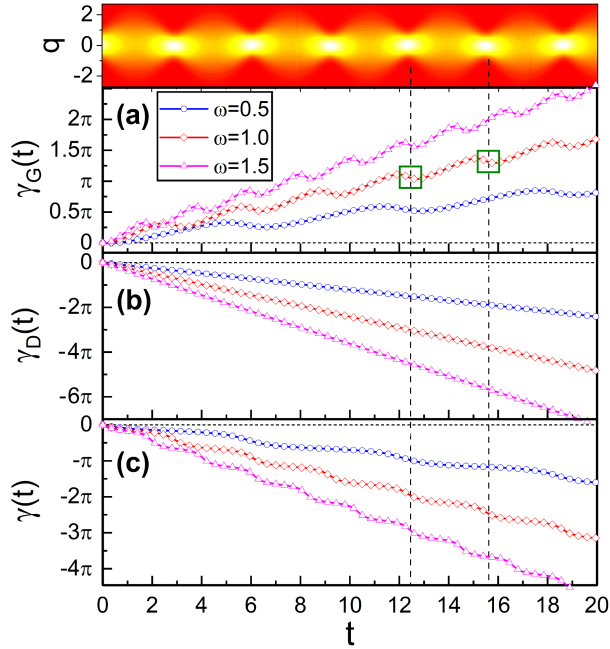


FIG. 3: Time evolution of the geometric phase **(a)**, dynamical phase **(b)**, and total phase **(c)** in the coherent state for several values of ω . For convenience of the related interpretation, density plot for the time evolution of the corresponding probability density with $\omega = 1$ is shown in the uppermost part. We have chosen the value of A_0 instead of Q_0 , i.e., we setted $A_0 = 0.1$: we will also specify the value of A_0 (not Q_0) in the subsequent figures for convenience from now on. We have used $c_1 = 2.5$, $c_2 = 0.5$, $t_0 = 0$, $\varphi = \theta = 0$, and $\gamma(t_0) = 0$ (that is, $\gamma_G(t_0) = \gamma_D(t_0) = 0$).

quadrature space (see the two rectangular regions in Fig. 3(a)). Such a fluctuational variation of the phase also becomes rapid as ω increases.

We see the effects of c_1 on the evolution of the geometric phase from Fig. 4. Because c_1 (together with c_2) is a factor that governs the measure of nonstaticity, the increment of the geometric phase becomes large as c_1 grows. Similar effects can also be confirmed when c_2 increases instead of c_1 (or when both c_1 and c_2 increase). Additionally, from the periodic pattern in the variation of three graphs in Fig. 4, we confirm that wave nonstaticity is revealed via the nonlinearity in the evolution of the geometric phase. Such a variation naturally disappears in the static limit (see the dash-dot line in lower part of Fig. 4).

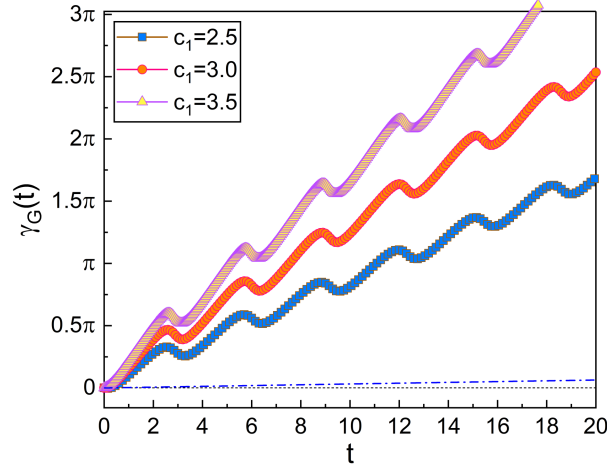


FIG. 4: Time evolution of the geometric phase in the coherent state for several values of c_1 . Because wave nonstaticity is governed by c_1 (and c_2), we can confirm the effects of nonstaticity on geometric phase from this figure. We have used $\omega = 1$, $A_0 = 0.1$, $c_2 = 0.5$ (except for an extra line), $t_0 = 0$, $\varphi = \theta = 0$, and $\gamma_G(t_0) = 0$. The measure of nonstaticity is 0.79, 1.02, and 1.22 in turn for the graphs designated in the legend. An extra line (dash-dot line) is the geometric phase without wave nonstaticity, i.e., for the case where $c_1 = c_2 = 1$ is chosen; this shows linear increase of the phase as mathematically turned up from Eq. (38).

5.2. Similarities and Differences with the Fock-State Phases

5.2.1. Harmonization with the dynamical phase

It may be worthwhile to compare the geometric phase in the coherent state to that in the Fock states considering the similarity of Eq. (43) with Eq. (44), which shows that A_0^2 in the coherent state plays a role similar to n in the Fock states. This consequence is closely related to the fact that $\langle A | \hat{A}^\dagger \hat{A} | A \rangle = A_0^2$ whereas $\langle \Phi_n | \hat{A}^\dagger \hat{A} | \Phi_n \rangle = n$. Regarding this, the evolution of the geometric phase in the coherent state is compared to that in the Fock states in Fig. 5 for several different values of c_2 while c_1 is taken to be a fixed value which is 5.000. This figure shows that the geometric phase in the coherent state increases as A_0^2 grows, whereas that in the Fock states increases as n grows. The average rate of such an increase in the coherent state is large when c_2 is large, while that in the Fock states is independent of c_2 in the case adopted

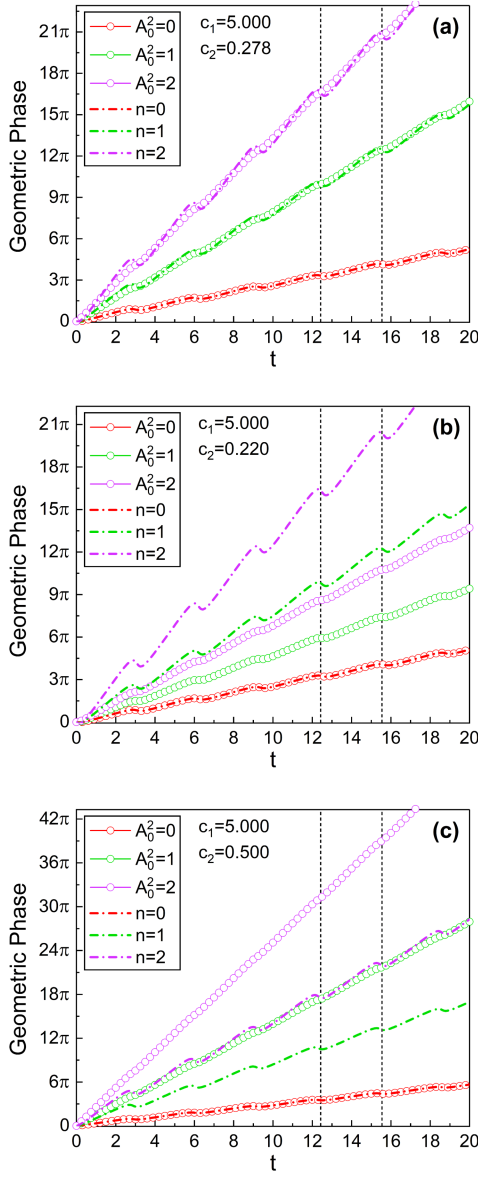


FIG. 5: Comparison of the evolution of the geometric phase ($\gamma_G(t)$, circles) in the coherent state with that ($\gamma_{G,n}(t)$, dash-dot lines) in the Fock states for $A_0^2 = n = 0$ (red), $A_0^2 = n = 1$ (green), and $A_0^2 = n = 2$ (violet). Two dotted vertical guidelines in each panel correspond to two adjacent nodes in the evolution of the nonstatic coherent wave like those in Fig. 3: this rule is also applied in subsequent figures up to Fig. 8. The values of (c_1, c_2) are $(5.000, 0.278)$ for (a), $(5.000, 0.220)$ for (b), and $(5.000, 0.500)$ for (c). We have used $\omega = 1$, $t_0 = 0$, $\varphi = \theta = 0$, and $\gamma_G(t_0) = \gamma_{G,n}(t_0) = 0$. The measure of nonstaticity is 1.73, 1.70, and 1.81 for the graphs in panels (a), (b), and (c), respectively.

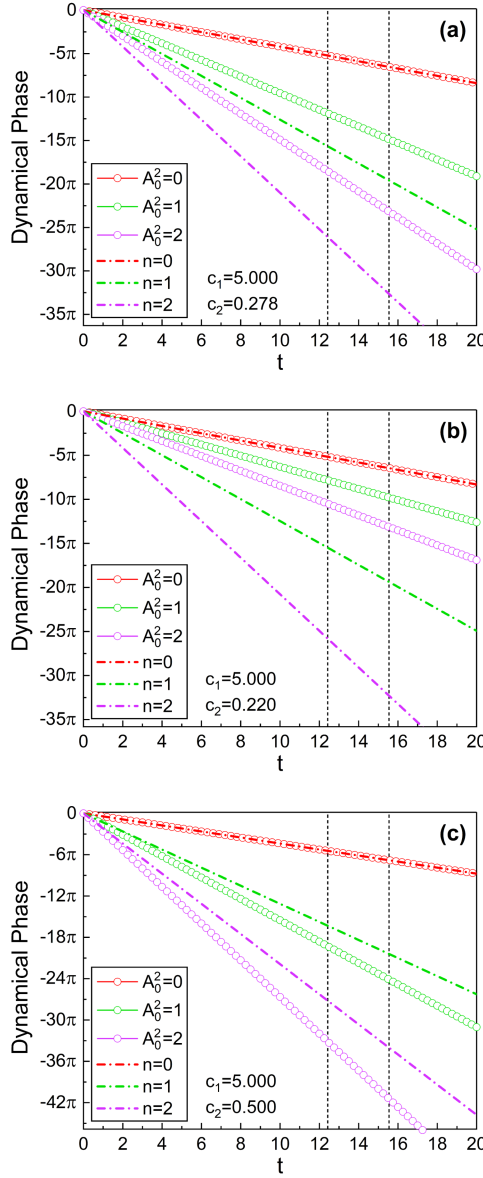


FIG. 6: Comparison of the evolution of the dynamical phase ($\gamma_D(t)$, circles) in the coherent state with that ($\gamma_{D,n}(t)$, dash-dot lines) in the Fock states for $A_0^2 = n = 0$ (red), $A_0^2 = n = 1$ (green), and $A_0^2 = n = 2$ (violet). The values of (c_1, c_2) are the same as those in Fig. 5 in turn for (a), (b), and (c), while $\gamma_D(t_0) = \gamma_{D,n}(t_0) = 0$ has been used. All of the other chosen parameters are also the same as those in Fig. 5.

in Fig. 5: this fact can be confirmed by comparing panels **(a)**, **(b)**, and **(c)** in Fig. 5 with one another regarding the differences in the scale of vertical axes. Figure 5**(a)** exhibits that the average rate of the increment of $\gamma_G(t)$ is the same as that of $\gamma_{G,n}(t)$ when c_2 is a specific value, which is 0.278. Figure 5**(b)** (Fig. 5**(c)**) shows that the average rate of the increment of $\gamma_G(t)|_{A_0^2=i}$ ($i = 1, 2$) is smaller (larger) than that of $\gamma_{G,n}(t)|_{n=i}$ provided that c_2 is smaller (larger) than 0.278.

On the other hand, we see from three panels of Fig. 5 that, for the case of $A_0^2 = n = 0$, $\gamma_G(t)$ is the same as $\gamma_{G,n}(t)$. It is also possible to show this fact analytically under the choice $\varphi = \theta = 0$. If we insert the formula of $\Gamma_D(\bar{t})$ given in Eq. (42) into Eq. (37) with the condition $A_0 = 0$, the geometric phase becomes

$$\gamma_G(t) = -\frac{1}{2}\omega T(t) + \omega \frac{c_1 + c_2}{4}[t - t_0] + \gamma_G(t_0). \quad (64)$$

This is the same as the zero-point Fock-state geometric phase $\gamma_{G,0}(t)$ that can be obtained from Eq. (E1) by setting $n = 0$ in addition to imposing a trivial condition $\gamma_G(t_0) = \gamma_{G,0}(t_0)$. For the case of $c_1 = c_2 \rightarrow 1$, the first term in the right hand side of Eq. (64) becomes $-\omega(t - t_0)/2$, leading to $\gamma_G(t)$ being zero provided that $\gamma_G(t_0) = 0$ as the initial condition. This outcome implies that the geometric phase disappears when its two sources are removed, i.e., it disappears when both the displacement and the nonstaticity are removed.

Figure 6 is the comparison of the evolution of $\gamma_D(t)$ with that of $\gamma_{D,n}(t)$, for several different values of c_2 like in the case of Fig. 5. $\gamma_D(t)$ is always the same as $\gamma_{D,n}(t)$ for the case of $A_0^2 = n = 0$: this consequence is quite similar to the case of the geometric phases and its analytical verification can also be done by the same way adopted in the case of those phases. However, the absolute values of $\gamma_D(t)|_{A_0^2=i}$ ($i = 1, 2$) are smaller than those of $\gamma_{G,n}(t)|_{n=i}$ for the case of Figs. 6**(a)** ($c_2 = 0.278$) and 6**(b)** ($c_2 = 0.220$), while the absolute values of $\gamma_D(t)|_{A_0^2=i}$ are larger than those of $\gamma_{G,n}(t)|_{n=i}$ for the case of Fig. 6**(c)** ($c_2 = 0.500$).

Figure 7 is the evolutions of the total phases, where the values of the nonstaticity measure are the same as those of Fig. 5, which are not so different from panel to panel. This figure shows that the dependency of the total phase on c_2 is negligible if the measures of nonstaticity are not much deviate from one another. However, since the phases in the nonstatic-wave evolutions are

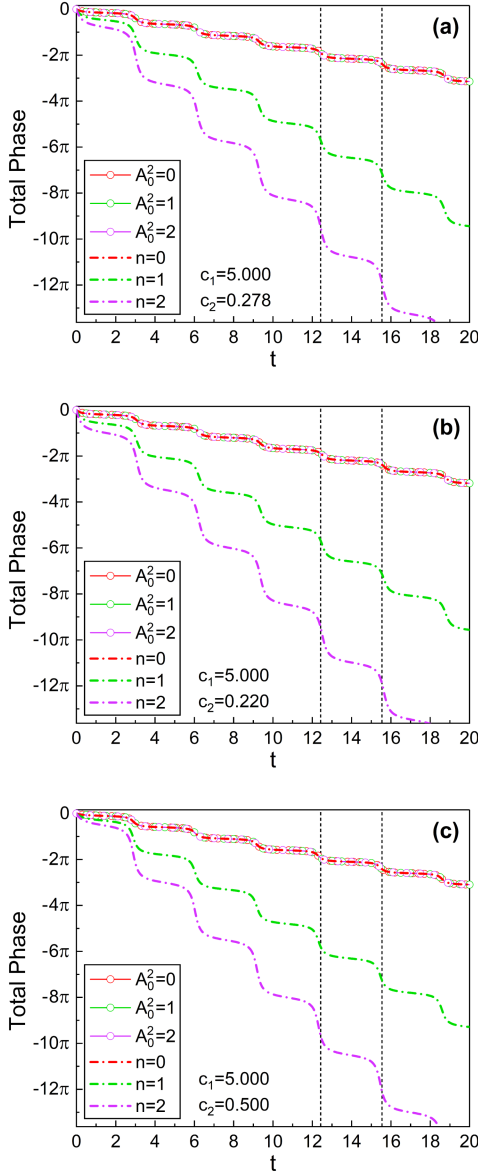


FIG. 7: Comparison of the evolution of the total phase ($\gamma(t)$, circles) in the coherent state with that ($\gamma_n(t)$, dash-dot lines) in the Fock states for $A_0^2 = n = 0$ (red), $A_0^2 = n = 1$ (green), and $A_0^2 = n = 2$ (violet). The values of (c_1, c_2) are the same as those in Fig. 5 in turn for (a), (b), and (c), while $\gamma(t_0) = \gamma_n(t_0) = 0$ has been used. All of the other chosen parameters are also the same as those in Fig. 5.

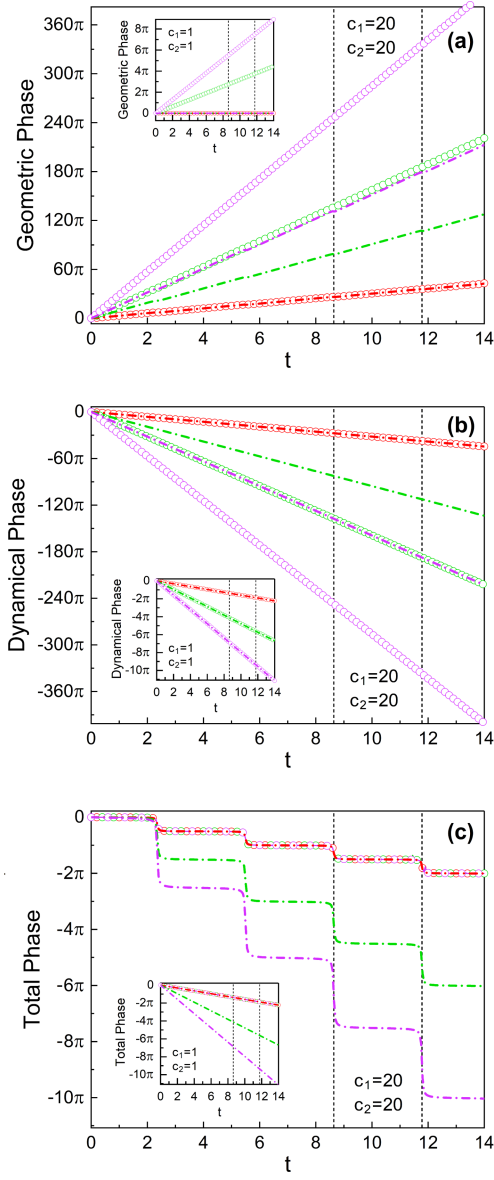


FIG. 8: The evolution of phases in the coherent (circles) and Fock (dash-dot lines) states for a light that has extreme nonstaticity: we have chosen $(c_1, c_2) = (20, 20)$ and this choice corresponds to the nonstaticity measure of $D = 14.12$. (a) is for $\gamma_G(t)$ and $\gamma_{G,n}(t)$, (b) is for $\gamma_D(t)$ and $\gamma_{D,n}(t)$, and (c) is for $\gamma(t)$ and $\gamma_n(t)$. The inset in each panel is in the limit of the static light-waves with the choice $(c_1, c_2) = (1, 1)$ for comparison. The rule for the values of A_0^2 and n is the same as that in Figs. 5, 6, and 7: that is, we choose $A_0^2 = n = 0$ (red), $A_0^2 = n = 1$ (green), and $A_0^2 = n = 2$ (violet). All chosen values of other parameters are also the same as those in Figs. 5, 6, and 7.

sensitive to the values of c_1 and c_2 (for example, compare the phases of light waves in the three panels of Fig. 2 in Ref. [17]), the phase $\gamma(t)$ (and $\gamma_n(t)$) in Fig. 7 is a little different from panel to panel. The phase in Fig. 7(b) (Fig. 7(c)) is slightly moved to the left (right) compared with that of Fig. 7(a). Of course, these minute phase shifts are also found in the geometric phase represented in Fig. 5. However, the scale of c_1 and c_2 does not affect the period of the nonlinear term, which is the first term in the right hand side of Eqs. (47) and (48). Such a period is dependent only on ω as can be seen from Fig. 3. That is, the period of the nonlinear evolution is small when ω is large and large when ω is small.

The similarity in the evolutions of the envelopes of the total phases in the three panels of Fig. 7 is noticeable, if we consider that the corresponding geometric-phase evolutions shown in Fig. 5 are very different from panel to panel. This consequence means that the evolutions of the geometric phases are harmonized with those of the dynamical phases in a way that the total phases are adjusted appropriately. As a consequence, the total phase in the coherent state is irrelevant to A_0 and always the same as that in the zero-point Fock state ($n = 0$).

5.2.2. Extreme nonstaticity limits

It may be instructive to see the phase evolutions for higher nonstatic waves, in addition to those that we have already seen from Figs. 5, 6, and 7. The phase evolutions with an extreme nonstaticity are represented in Fig. 8 with the choice of $c_1 = c_2 = 20$. While the measure of nonstaticity in this case is $D = 14.12$, the evolutions of phases in the static-wave limit ($D = 0$) are also given in insets in Fig. 8 for a comparison purpose. Figure 8(a) exhibits that the geometric phase evolves nearly linearly under this gigantic nonstaticity. Although the nonlinear term $\gamma_{G,NL}(t)$ in Eq. (47) is being seriously distorted as the measure of nonstaticity increases, its contribution to the total phase becomes relatively small with the grow of the nonstaticity because the scale of the linear term $\gamma_{G,L}(t)$ highly increases at the same time. $\gamma_{G,L}(t)$ becomes dominant in this way and, thereby, the nonlinear-term-induced distortion in the geometric-phase evolution is buried in the linear-term outcome as the nonstaticity becomes such a very high value. This is the reason why the graphs in Fig. 8(a) looks like almost linear in spite of the significant distortion of the part associated to its nonlinear-term. The geometric

phase in the coherent state is not zero even when the nonstaticity disappears, except for the case of $A_0^2 = 0$, as we have confirmed previously. However, the inset in Fig. 8(a) exhibits that the geometric phases in the Fock states are in contrast always zero provided that the nonstaticity disappears. Recall that the wave nonstaticity is the only source of appearing the geometric phase for the case of the non-displaced Fock states considered here.

Figure 8(b) shows that the increase of the absolute values of the dynamical phases over time is conspicuously small for the case of Fock states compared to that of the coherent state. However, we confirm from the inset in Fig. 8(b) that that increment becomes the same as that in the coherent state in the static-wave limit: notice that the structural equality between Eqs. (43) and (44) mathematically supports this consequence. It looks like, from Fig. 8(b), that $\gamma_D(t)$ with $A_0^2 = 1$ is the same as $\gamma_{D,n}(t)$ with $n = 2$. To see this outcome in detail, we consider the approximate value of the geometric phase in the coherent state utilizing Eq. (35) with Eq. (42) in the limit $c_1 = c_2 \gg 1$ with $\gamma_D(t_0) = 0$:

$$\gamma_D(t) \approx -\omega \left(2A_0^2 + \frac{1}{2} \right) c_1(t - t_0), \quad (65)$$

which is the same as the exact value of $\gamma_{D,n}(t)$ given in Eq. (E2) in the same limit, provided that $A_0^2 = n/2$ and $\gamma_{D,n}(t_0) = 0$. Hence, $\gamma_D(t)$ with the choice $A_0^2 = 1$ in the case of a highly nonstatic wave is very the same as $\gamma_{D,n}(t)$ with $n = 2$ as also confirmed graphically.

The harmonized evolution of the dynamical phases given in Fig. 8(b) makes the total phases (Fig. 8(c)) similar to those in Fig. 7, except for the prominence of their strange nonlinear behavior. We see from Fig. 8(c) that the total phases abruptly drop at the nodes in the periodic nonstatic-wave evolutions. Whereas their evolving patterns are fairly different compared to those in Fig. 7, this outcome is evidently due to the greatness of the measure of nonstaticity. Such precipitations in the graphs however entirely disappear in the static-wave limit, forming their evolutions being linear (see inset of Fig. 8(c)). By the way, the average gradient in the evolution of the total phase and the period of its nonlinear portion are different depending on ω as it can be checked from Fig. 3(c).

5.2.3. More detailed comparison with the Fock-state geometric phases

More detailed dependence of the geometric phase on c_1 and c_2 can be seen from Fig. 9. We can

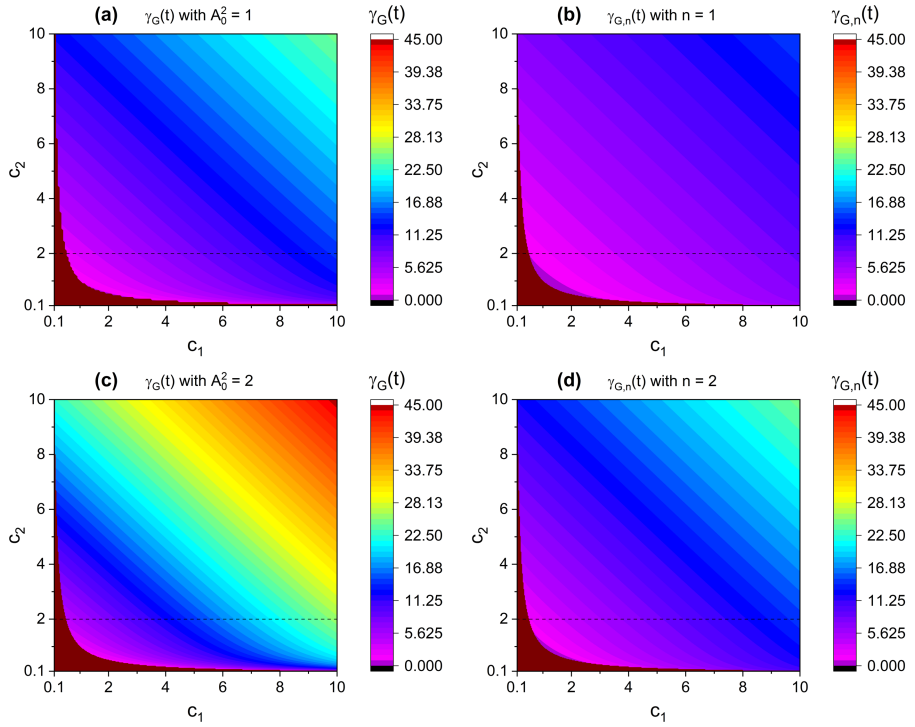


FIG. 9: Density plots for the geometric phases in the coherent and Fock states depending on c_1 and c_2 : (a) is $\gamma_G(t)$ with $A_0^2 = 1$, (b) is $\gamma_{G,n}(t)$ with $n = 1$, (c) is $\gamma_G(t)$ with $A_0^2 = 2$, and (d) is $\gamma_{G,n}(t)$ with $n = 2$. We considered the geometric phases evolved during a unit time by choosing $t_0 = 0$ and $t = 1$. The dark reddish brown region in the lower left corner of each panel is invalid/noncalculable region according to the condition given in Eq. (5). We used $\omega = 1$, $\varphi = \theta = 0$, and $\gamma_G(t_0) = 0$.

see from this figure that the increase of the geometric phase in a unit time is large when both c_1 and c_2 are high for both the coherent and the Fock states. Figure 10 is the comparison of the geometric phase along the dashed lines in Fig. 9. All four graphs of the geometric phase in this figure increase almost monotonically as c_1 grows. We have also confirmed similar increase of the geometric phase along with the increase of c_2 (not shown). This consequence means that the wave nonstaticity, which is determined by c_1 and c_2 , is the main factor that is responsible for the advent of the geometric phase (or enhancement of an existing geometric phase when, for example, $A_0 \neq 0$ in the coherent state).

By the way, Fig. 9 together with Fig. 10 shows that, as the degree of nonstaticity increases,

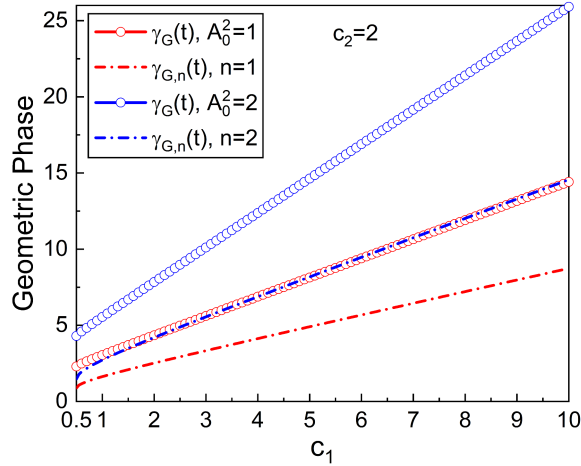


FIG. 10: Comparison of the geometric phase along the dashed lines in each panel of Fig. 9. That is, the variation of the geometric phases depending on c_1 for four specific cases where we have chosen $c_2 = 2$: they are $\gamma_G(t)$ with $A_0^2 = 1$ (red circle line) and $A_0^2 = 2$ (blue circle line), and $\gamma_{G,n}(t)$ with $n = 1$ (red dash-dot line) and $n = 2$ (blue dash-dot line). We considered only the valid value as the initial value of c_1 in the horizontal axis according to the restriction of Eq. (5): $c_1 \geq 0.5$. We used the values of parameters given in Fig. 9, i.e., $\omega = 1$, $t_0 = 0$, $t = 1$, $\varphi = \theta = 0$, and $\gamma_G(t_0) = 0$.

the geometric phase in the case of the coherent state is more dominant rather than that in the Fock states: while this is the usual consequence confirmable based on Fig. 9 for most choices of c_1 and c_2 , an exception is the case given in Fig. 5(b). Regarding this consequence, we have shown the dependence of the geometric phase on A_0^2 (for the coherent state) and n (for Fock states) in Fig. 11. Though A_0^2 in the coherent state plays the role similar to n in the Fock states in a sense that the increase of the geometric phase over time is controlled by them almost in the same manner, the two factors are physically different from each other as it is known. A_0^2 determines the scale of displacement in the coherent state, while n determines energy level in the Fock states. We conclude from Fig. 11(a1) that the geometric phase is usually more significantly affected by the displacement rather than the increase of the energy level when $\varphi = \theta = 0$, whereas Fig. 11(a2) shows an exceptional case. Figure 11(b) however manifests that this consequence does not hold if we choose other values of φ and θ . Meanwhile,

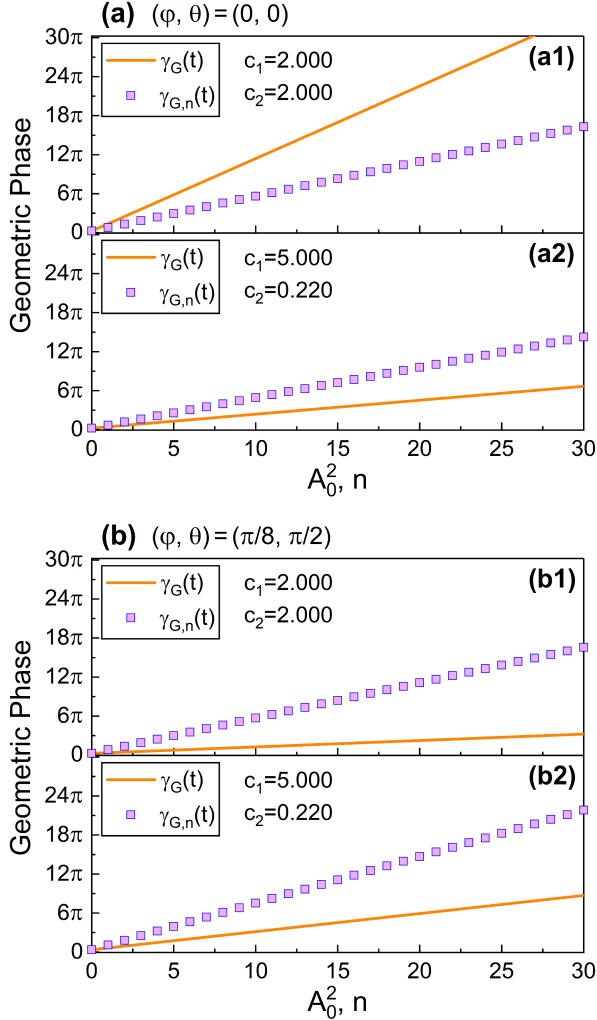


FIG. 11: The dependence of the geometric phases $\gamma_G(t)$ and $\gamma_{G,n}(t)$ evolved over unit time on A_0^2 (for $\gamma_G(t)$) and n (for $\gamma_{G,n}(t)$), where $(\varphi, \theta) = (0, 0)$ for (a) and $(\varphi, \theta) = (\pi/8, \pi/2)$ for (b). $t_0 = 0$ and $t = 1$ have been taken in this figure to adopt the unit-time interval. We have chosen $(c_1, c_2) = (2.000, 2.000)$ for subpanels (a1) and (b1) and $(c_1, c_2) = (5.000, 0.220)$ for (a2) and (b2), while $\omega = 1$ and $\gamma_G(t_0) = \gamma_{G,n}(t_0) = 0$ are used.

the geometric phase in a non-displaced coherent state ($A_0^2 = 0$) is exactly the same as that in the zero-point Fock state provided that $\varphi = \theta = 0$ as previously expected according to Eq. (64).

6. CONCLUSION

The geometric phase of a nonstatic light in the coherent state, arisen in a static environment, has been investigated by adopting a generalized annihilation operator \hat{A} . \hat{A} is represented in terms of the nonlinear time function $f(t)$ that is controlled by the nonstaticity parameters c_1 and c_2 . We introduced a time-varying nonstatic wave function, which is the eigenfunction of \hat{A} . Then, the geometric phase associated with the wave nonstaticity was evaluated by utilizing that wave function.

Our general geometric phase showed nonlinear variation due to the consideration of wave nonstaticity. A regular pattern in the variation of the geometric phase has been recognized: we have analyzed it in detail along with examining the effects of the overall phase caused by the peculiar behavior of the geometric phase as its component. The evolution of the geometric phase in time is a combination of its linear increase and a sinusoidal-like fluctuation. The fluctuation in the evolving of phase is raised from the nonlinearity of $f(t)$ accompanying the wave nonstaticity. The increment of the geometric phase over time becomes rapid when c_1 and c_2 become large. Such increment in the coherent state is quite drastic in most cases compared to that in the Fock states. We confirmed that the angular frequency ω and amplitude A_0 also affect the pattern in the phase evolutions. For instance, the frequency of the nonlinear portion in the geometric-phase fluctuation is relatively high when ω is large.

The evolution of the geometric phase is harmonized with the dynamical phase, leading to the time-averaged incrementing rate of the total phase being not affected by the magnitude of wave nonstaticity. Notably, the scale of distortion in the total phase is determined only by the nonstaticity measure, while the average gradient of the total phase and the period of its nonlinear portion are determined by ω . For the case of an extreme nonstaticity, the nonlinear portion of the geometric phase undergoes a great distortion and, thereby, the total phase exhibits a unique and singular pattern in its evolution. That is, total phase abruptly drops whenever the wave forms a node periodically over time. However, in the limit of $f(t) = 1$, the fluctuation of the geometric phase disappears, showing only its linear increase. The remaining rate of the geometric-phase increase over time corresponds only to the elemental part in this

limit. Namely, the nonstaticity-induced portion in such a linear increment no longer exists.

It was demonstrated that the nonstatic wave function in the coherent state satisfies the Schrödinger equation only when we consider the geometric phase as an additional phase to the dynamical one. This fact means that the emergence of the geometric phase is essential when the wave exhibits nonstaticity. The geometric phase is one of the most fundamental elements in quantum mechanics in connection with a nonstatic-wave evolution and parallel transport of the state. Exact mathematical formulation of the geometric phase in the generalized coherent state achieved in this work is necessary not only for extending our knowledge in this field, but for pursuing further studies in relation with nonstatic light rigorously as well. Characterizing profound properties of the geometric phase is important for its substantial utilization in diverse emerging scientific fields, such as the quantum information technology, metamaterials-based photonic devices, light control for Holograms, and detectors for gravitational waves [41–43].

Appendix A: Full version of the coherent-state expansion over Fock states

It is possible to represent the wave function in the coherent state in the manner of Eq. (12) instead of Eq. (13). That is, regarding Eqs. (9), (13), and (46), we have

$$\langle q | \Psi_{\text{coh}}(t) \rangle = \sum_{n=0}^{\infty} a_n \langle q | \Psi_n(t) \rangle, \quad (\text{A1})$$

where a_n in this case take the form

$$\begin{aligned} a_n &= b_n(A) \exp\{-i[\gamma_n(t) - \gamma(t)]\} \\ &= \exp(-A_0^2/2) \frac{A_0^n}{\sqrt{n!}} \exp\{-i[\gamma_n(t_0) - \gamma(t_0)] - in\theta\}, \end{aligned} \quad (\text{A2})$$

whereas A_0 and θ are constants over time, which appear in Eq. (15). In the derivation of the last formula in Eq. (A2), we used Eqs. (15), (45), and (E3). Note that Eq. (A2) does not vary in time.

Appendix B: Gauge invariance of the geometric phase

To show the gauge invariance property of the geometric phase, let us consider a model of U1 gauge transformation for the full wave function $|\Psi_{\text{coh}}(t)\rangle$ given in Eq. (46). We represent such a transformation as

$$|\tilde{\Psi}_{\text{coh}}(t)\rangle = e^{i\alpha(t)}|\Psi_{\text{coh}}(t)\rangle, \quad (\text{B1})$$

where $\alpha(t)$ is an arbitrary time-dependent phase. To tackle our problem of the demonstration in connection with Eq. (B1), we rewrite the geometric phase represented in Eq. (22) such that [7]

$$\gamma_G(t) = \arg(\langle \Psi_{\text{coh}}(t_0) | \Psi_{\text{coh}}(t) \rangle) + \int_{t_0}^t \langle \Psi_{\text{coh}}(t') | i \frac{\partial}{\partial t'} | \Psi_{\text{coh}}(t') \rangle dt' + \gamma_G(t_0). \quad (\text{B2})$$

It is not difficult to prove that this formula of the geometric phase is the same as Eq. (22) using the relation given in Eq. (46).

Then the geometric phase related to $|\tilde{\Psi}_{\text{coh}}(t)\rangle$ can be written in the form

$$\begin{aligned} \tilde{\gamma}_G(t) &= \arg(\langle \tilde{\Psi}_{\text{coh}}(t_0) | \tilde{\Psi}_{\text{coh}}(t) \rangle) + \int_{t_0}^t \langle \tilde{\Psi}_{\text{coh}}(t') | i \frac{\partial}{\partial t'} | \tilde{\Psi}_{\text{coh}}(t') \rangle dt' + \gamma_G(t_0) \\ &\equiv I_1 + I_2 + \gamma_G(t_0), \end{aligned} \quad (\text{B3})$$

where I_1 and I_2 indicate merely the first and second terms of the mathematical expression in the former line, respectively. We have assumed $\tilde{\gamma}_G(t_0) = \gamma_G(t_0)$ in the above expression for simplicity. Minor evaluations using Eq. (B1) give

$$I_1 = \arg(\langle \Psi_{\text{coh}}(t_0) | \Psi_{\text{coh}}(t) \rangle) + \alpha(t) - \alpha(t_0), \quad (\text{B4})$$

$$I_2 = - \int_{t_0}^t \dot{\alpha}(t') dt' + \int_{t_0}^t \langle \Psi_{\text{coh}}(t') | i \frac{\partial}{\partial t'} | \Psi_{\text{coh}}(t') \rangle dt'. \quad (\text{B5})$$

Using the relation $\int_{t_0}^t \dot{\alpha}(t') dt' = \alpha(t) - \alpha(t_0)$ in connection with I_2 , we now immediately confirm that $\tilde{\gamma}_G(t) = \gamma_G(t)$. Thus the geometric phase is invariant under the considered transformation of the gauge.

Appendix C: Intermediate steps in evaluating phases

We first represent the methods for obtaining the coefficients $g_1(t)$ - $g_4(t)$ appeared in Eqs. (27)-(30) as the factors of the geometric phase. By evaluating Eq. (22) with the use of Eq. (24), the geometric phase becomes Eq. (25) with

$$g_1(t) = -\frac{1}{f(t)}(A^2 + A^{*2} - 2A^*A + 1), \quad (C1)$$

$$g_2(t) = \frac{[\dot{f}(t)]^2}{f(t)}(A^2 + A^{*2} + 2A^*A + 1), \quad (C2)$$

$$g_3(t) = \frac{i\dot{f}(t)}{f(t)}(-A^2 + A^{*2}), \quad (C3)$$

$$g_4(t) = f(t)(A^2 + A^{*2} + 2A^*A + 1). \quad (C4)$$

Now minor arrangements after substituting Eq. (15) into the above equations lead to Eqs. (27)-(30) in the text.

In addition, we see the method for obtaining $\bar{g}_1(t)$ in Eq. (34), which is a coefficient needed for expressing the dynamical phase. A straightforward evaluation of Eq. (23) gives an intermediate formula of the dynamical phase, which is Eq. (32) with Eqs. (C2)-(C4) and

$$\bar{g}_1(t) = -\frac{1}{f(t)}(A^2 + A^{*2} - 2A^*A - 1). \quad (C5)$$

Then, by managing the above equation with the use of Eq. (15), we have the eventual formula of $\bar{g}_1(t)$ which is Eq. (34).

Appendix D: Verification that $\Gamma_D(t)$ is a time constant

To verify that $\Gamma_D(t)$ in Eq. (33) is a time constant, we see its time derivative. An explicit evaluation with Eq. (33) yields

$$\begin{aligned} \frac{d\Gamma_D(t)}{dt} = & \left[\omega^2 - \frac{1}{f^2(t)} \left(\omega^2 + \frac{[\dot{f}(t)]^2}{4} \right) + \frac{\ddot{f}(t)}{2f(t)} \right] \left(A_0^2 \sin[2(\omega T(t) + \theta)] \right. \\ & \left. - \frac{\dot{f}(t)}{4\omega} [1 + 4A_0^2 \cos^2(\omega T(t) + \theta)] \right). \end{aligned} \quad (D1)$$

We applied the relation in Eq. (59) and utilized the fact that A_0 is a time-constant (i.e., $dA_0/dt = 0$) in the derivation of this equation. Now by replacing $\ddot{f}(t)$ in the above equation with Eq. (60), we readily have $d\Gamma_D(t)/dt = 0$. Hence, $\Gamma_D(t)$ is constant over time.

Appendix E: Geometric, dynamical, and total phases in the Fock states

The geometric phase, the dynamical phase, and the total phase in the Fock states with nonstaticity are given by [18]

$$\gamma_{G,n}(t) = \left(n + \frac{1}{2}\right) \left(\frac{c_1 + c_2}{2}\omega(t - t_0) - \omega T(t)\right) + \gamma_{G,n}(t_0), \quad (\text{E1})$$

$$\gamma_{D,n}(t) = -\left(n + \frac{1}{2}\right) \frac{c_1 + c_2}{2}\omega(t - t_0) + \gamma_{D,n}(t_0), \quad (\text{E2})$$

$$\gamma_n(t) = -\left(n + \frac{1}{2}\right)\omega T(t) + \gamma_n(t_0), \quad (\text{E3})$$

for $t \geq t_0$.

[1] P. A. M. Dirac, “Quantised singularities in the electromagnetic field,” Proc. Roy. Soc. Lond. A **133**(821), 60–72 (1931). DOI: 10.1098/rspa.1931.0130.

[2] T. V. Mechelen and Z. Jacob, “Photonic Dirac monopoles and skyrmions: spin-1 quantization,” Opt. Mater. Express **9**(1), 95–111 (2019). DOI: 10.1364/OME.9.000095.

[3] M. V. Berry, “Quantal phase factors accompanying adiabatic changes,” Proc. R. Soc. Lond. A **392**(1802), 45–57 (1984). DOI: 10.1098/rspa.1984.0023.

[4] W. Zhao and X. Wang, “Berry phase in quantum oscillations of topological materials,” Adv. Phys. X, **7**(1), 2064230 (2022). DOI: 10.1080/23746149.2022.2064230.

[5] Y. Aharonov and J. Anandan, “Phase change during a cyclic quantum evolution,” Phys. Rev. Lett. **58**(16), 1593–1596 (1987). DOI: 10.1103/PhysRevLett.58.1593.

[6] C. Bengs, M. Sabba, and M. H. Levitt, “The Aharonov–Anandan phase and geometric double-quantum excitation in strongly coupled nuclear spin pairs,” *J. Chem. Phys.* **158**(12), 124204 (2023). DOI: 10.1063/5.0138146.

[7] N. Mukunda and R. Simon, “Quantum kinematic approach to the geometric phase. I. General formalism,” *Ann. Phys.* **228**(2), 205–268 (1993). DOI: 10.1006/aphy.1993.1093.

[8] A.-B. A. Mohamed and I. Masmali, “Control of the geometric phase in two open qubit–cavity systems linked by a waveguide,” *Entropy* **22**(1), 85 (2020). DOI: 10.3390/e22010085.

[9] L. Garza-Soto, N. Hagen, D. Lopez-Mago, and Y. Otani, “Differences between the geometric phase and propagation phase: clarifying the boundedness problem,” *Appl. Opt.* **63**(3), 645–653 (2024). DOI: 10.1364/AO.510509.

[10] B. Simon, “Holonomy, the quantum adiabatic theorem, and Berry’s phase,” *Phys. Rev. Lett.* **51**(24), 2167–2170 (1983). DOI: 10.1103/PhysRevLett.51.2167.

[11] K. Y. Bliokh, M. A. Alonso, and M. R. Dennis, “Geometric phases in 2D and 3D polarized fields: geometrical, dynamical, and topological aspects,” *Rep. Prog. Phys.* **82**(12), 122401 (2019). DOI: 10.1088/1361-6633/ab4415.

[12] M. Maamache, “Ermakov systems, exact solution, and geometrical angles and phases,” *Phys. Rev. A* **52**(2), 936–940 (1995). DOI: 10.1103/PhysRevA.52.936.

[13] J. Zhang, T. H. Kyaw, S. Philipp, L.-C. Kwek, E. Sjöqvist, and D. Tong, “Geometric and holonomic quantum computation,” *Phys. Rep.* **1027**, 1–53 (2023). DOI: 10.1016/j.physrep.2023.07.004.

[14] G. F. Xu and D. M. Tong, “Realizing multi-qubit controlled nonadiabatic holonomic gates with connecting systems,” *AAPPS Bull.* **32**(1), 13 (2022). DOI: 10.1007/s43673-022-00043-6.

[15] Y.-H. Lee, G. Tan, T. Zhan, Y. Weng, G. Liu, F. Gou, F. Peng, N. V. Tabiryan, S. Gauza, and S.-T. Wu, “Recent progress in Pancharatnam-Berry phase optical elements and the applications for virtual/augmented realities,” *Opt. Data Process. Storage* **3**(1), 79–88 (2017). DOI: 10.1515/odps-2017-0010.

[16] J. Lee, Y. Kim, K. Choi, J. Hahn, S.-W. Min, and H. Kim, “Digital incoherent compressive holography using a geometric phase metalens,” *Sensors* **21**(16), 5624 (2021). DOI: 10.3390/s21165624.

[17] J. R. Choi, “On the possible emergence of nonstatic quantum waves in a static environment,” *Phys. Rev. Lett.* **127**(12), 120401 (2021). DOI: 10.1103/PhysRevLett.127.120401.

ment,” *Nonlinear Dyn.* **103**(3), 2783–2792 (2021). DOI: 10.1007/s11071-021-06222-8.

[18] J. R. Choi, “Effects of light-wave nonstaticity on accompanying geometric-phase evolutions,” *Opt. Express* **29**(22), 35712–35724 (2021). DOI: 10.1364/OE.440512.

[19] J. R. Choi, K. H. Yeon, I. H. Nahm, and S. S. Kim, “Do the generalized Fock-state wave functions have some relations with classical initial condition?” *Pramana-J. Phys.* **73**(5), 821–828 (2009). DOI: 10.1007/s12043-009-0150-4.

[20] J. R. Choi, “Analysis of light-wave nonstaticity in the coherent state,” *Sci. Rep.* **11**, 23974 (2021). DOI: 10.1038/s41598-021-03047-8.

[21] A. Mostafazadeh, “Quantum adiabatic approximation, quantum action, and Berry’s phase,” *Phys. Lett. A* **232**(6), 395–398 (1997). DOI: 10.1016/S0375-9601(97)00391-5.

[22] G. McCaul, A. Pechen, and D. I. Bondar, “Entropy non-conservation and boundary conditions for Hamiltonian dynamical systems,” *Phys. Rev. E* **99**(6), 062121 (2019). DOI: 10.1103/PhysRevE.99.062121.

[23] O. V. Usatenko, J.-P. Provost, and G. Vallée, “A comparative study of the Hannay’s angles associated with a damped harmonic oscillator and a generalized harmonic oscillator,” *J. Phys. A* **29**(10), 2607–2610 (1996). DOI 10.1088/0305-4470/29/10/035.

[24] J. Y. Zeng and Y. A. Lei, “Connection between the Berry phase and the Lewis phase,” *Phys. Lett. A* **215**(5-6), 239–244 (1996). DOI: 10.1016/0375-9601(96)00254-X.

[25] P. Martin-Dussaud, “Searching for coherent states: From origins to quantum gravity,” *Quantum* **5**, 390 (2021). DOI: 10.22331/q-2021-01-28-390.

[26] R. J. Glauber, “Coherent and incoherent states of the radiation field,” *Phys. Rev.* **131**(6), 2766–2788 (1963). DOI: 10.1103/PhysRev.131.2766.

[27] W. Schleich and J. A. Wheeler, “Oscillations in photon distribution of squeezed states and interference in phase space,” *Nature* **326**(6113), 574–577 (1987). DOI: 10.1038/326574a0.

[28] R. Lynch, “Simultaneous fourth-order squeezing of both quadrature components,” *Phys. Rev. A* **49**(4), 2800–2805 (1994). DOI: 10.1103/PhysRevA.49.2800.

[29] Y. Wang, H. Ye, Z. Yu, Y. Liu, and W. Xu, “Sub-Poissonian photon statistics in quantum dot-metal nanoparticles hybrid system with gain media,” *Sci. Rep.* **9**, 10088 (2019). DOI:

10.1038/s41598-019-46576-z.

- [30] W. H. Louisell, *Quantum Statistical Properties of Radiation* (John Wiley and Sons, New York, 1973), p. 105.
- [31] N. E. Gürbüz, “Three geometric phases with the visco-Da Rios equation for the hybrid frame in R_1^3 ,” *Optik* **248**, 168116 (2021). DOI: 10.1016/j.ijleo.2021.168116.
- [32] H. Kuratsuji and S. Iida, “Effective action for adiabatic process: dynamical meaning of Berry and Simon’s phase,” *Prog. Theor. Phys.* **74**(3), 439–445 (1985). DOI: 10.1143/PTP.74.439.
- [33] L. Koens and E. Lauga, “Geometric phase methods with Stokes theorem for a general viscous swimmer,” *J. Fluid Mech.* **916**, A17 (2021). DOI: 10.1017/jfm.2021.181.
- [34] P. C. Deshmukh, S. Ghosh, U. Kumar, C. Hareesh, and G. Aravind, “A primer on path integrals, Aharonov–Bohm effect and the geometric phase,” *Phys. Educ.* **4**(1), 2250005 (2022). DOI: 10.1142/S2661339522500056.
- [35] S. N. Biswas and S. K. Soni, “Berry’s phase for coherent states and canonical transformation,” *Phys. Rev. A* **43**(10), 5717–5719 (1991). DOI: 10.1103/PhysRevA.43.5717.
- [36] J. Grain and V. Vennin, “Canonical transformations and squeezing formalism in cosmology,” *J. Cosmol. Astropart. Phys.* **2020**(2), 022 (2020). DOI 10.1088/1475-7516/2020/02/022.
- [37] S. Chaturvedi, M. S. Sriram, and V. Srinivasan, “Berry’s phase for coherent states,” *J. Phys. A: Math. Gen.* **20**(16), L1071–L1075 (1987). DOI 10.1088/0305-4470/20/16/007.
- [38] J. R. Choi, “Quadrature squeezing and geometric-phase oscillations in nano-optics,” *Nanomaterials* **10**(7), 1391 (2020). DOI: 10.3390/nano10071391.
- [39] W. Ding and Z. Wang, “‘Classical’ coherent state generated by curved surface,” *New J. Phys.* **24**, 113002 (2022). DOI 10.1088/1367-2630/ac9a9e.
- [40] E. Munguía-González, S. Rego, and J. K. Freericks, “Making squeezed-coherent states concrete by determining their wavefunction,” *Am. J. Phys.* **89**(9), 885–896 (2021). DOI: 10.1119/10.0004872.
- [41] J. Zhang, T. H. Kyaw, S. Philipp, L.-C. Kwek, E. Sjöqvist, and D. Tong, “Geometric and holonomic quantum computation,” *Phys. Rep.* **1027**, 1–53 (2023). DOI: 10.1016/j.physrep.2023.07.004.
- [42] C. P. Jisha, S. Nolte, and A. Alberucci, “Geometric phase in Optics: from wavefront manipulation to waveguiding,” *Laser Photonics Rev.* **15**(10), 2100003 (2021). DOI: 10.1002/lpor.202100003.

[43] I. L. Paiva, R. Lenny, and E. Cohen, “Geometric phases and the Sagnac effect: foundational aspects and sensing applications,” *Adv. Quantum Technol.* **5**(2), 2100121 (2022). DOI: 10.1002/qute.202100121.